

Reactivated spatial context guides episodic recall

Nora A. Herweg¹, Ashwini D. Sharan², Michael R. Sperling³, Armin Brandt⁴, Andreas Schulze-Bonhage⁴, Michael J. Kahana^{1,5}

¹ Computational Memory Lab, Department of Psychology, University of Pennsylvania, Philadelphia, PA, USA

² Department of Neurosurgery, Thomas Jefferson University Hospital, Philadelphia, PA, USA

³ Department of Neurology, Thomas Jefferson University, Philadelphia, PA, USA

⁴ Epilepsy Center, University Medical Center, Freiburg, Germany

⁵ Lead contact

* Correspondence:

Dr. Nora A Herweg

nherweg@sas.upenn.edu

or

Dr. Michael J Kahana

kahana@psych.upenn.edu

Keywords: spatial memory; reinstatement; theta; gamma; hippocampus; parahippocampal gyrus; MTL; intracranial

25 **Abstract**

26 The medial temporal lobe (MTL) is known as the locus of spatial coding and episodic memory,
27 but the interaction between these cognitive domains, as well as the extent to which they rely on
28 common neurophysiological mechanisms is poorly understood. Here, we use a hybrid spatial-
29 episodic memory task to determine how spatial information is dynamically reactivated in sub-
30 regions of the MTL and how this reactivation guides recall of episodic information. Our results
31 implicate theta oscillations across the MTL as a common neurophysiological substrate for spatial
32 coding in navigation and episodic recall. We further show that spatial context information is
33 initially retrieved in the hippocampus (HC) and subsequently emerges in the parahippocampal
34 gyrus (PHG). Finally, we demonstrate that hippocampal theta phase modulates parahippocampal
35 gamma amplitude during retrieval of spatial context, suggesting a role for cross frequency coupling
36 in coding and transmitting retrieved spatial information.

37 **Introduction**

38 Spatio-temporal context provides a unique tag for each event we experience, and the
39 similarities among these contextual tags serve to organize the contents of episodic memory. This
40 organization cannot be observed directly but can be inferred from the way people recall
41 information. When remembering lists of words, people exhibit a robust tendency to successively
42 recall words that occurred in neighboring list positions [1,2]. While most studies on episodic
43 memory focused on this *temporal contiguity* effect, more recent research has shown that spatial
44 context similarly guides recall transitions. During recall of items presented in a 3D virtual
45 environment, subjects showed a *spatial contiguity* effect, successively recalling items studied at
46 proximate locations in the environment [3]. These results suggest that both temporal and spatial
47 context reactivate during recall and cue associated items. They further establish a direct link
48 between spatial coding and episodic memory, two cognitive domains that have been associated
49 with the medial temporal lobe (MTL) in parallel lines of research.

50 During navigation, single cells in the hippocampus (HC) and entorhinal cortex represent
51 current spatial location with a single place field (i.e. place cells) [4,5] or multiple place fields
52 arranged in a hexagonal grid (i.e. grid cells) [6,7], respectively. These firing patterns are
53 accompanied by hippocampal low frequency oscillations in the delta to theta band which can
54 appear in raw traces and manifest in increased spectral power during movement compared to
55 stillness [8–16]. In rodents a direct relationship between the two phenomena has been observed:
56 Place cells fire at progressively earlier phases of the theta cycle, as a rat traverses a place field
57 [17]. Moreover, grid cell firing can be silenced by inhibiting theta oscillations [18,19] (although
58 grid cells have also been observed in bats in the absence of continuous theta oscillations [20]). In
59 humans, increased delta-theta power during navigation, immediately preceding navigation or
60 during a cued location memory task has been linked to navigation performance [10,13] and spatial

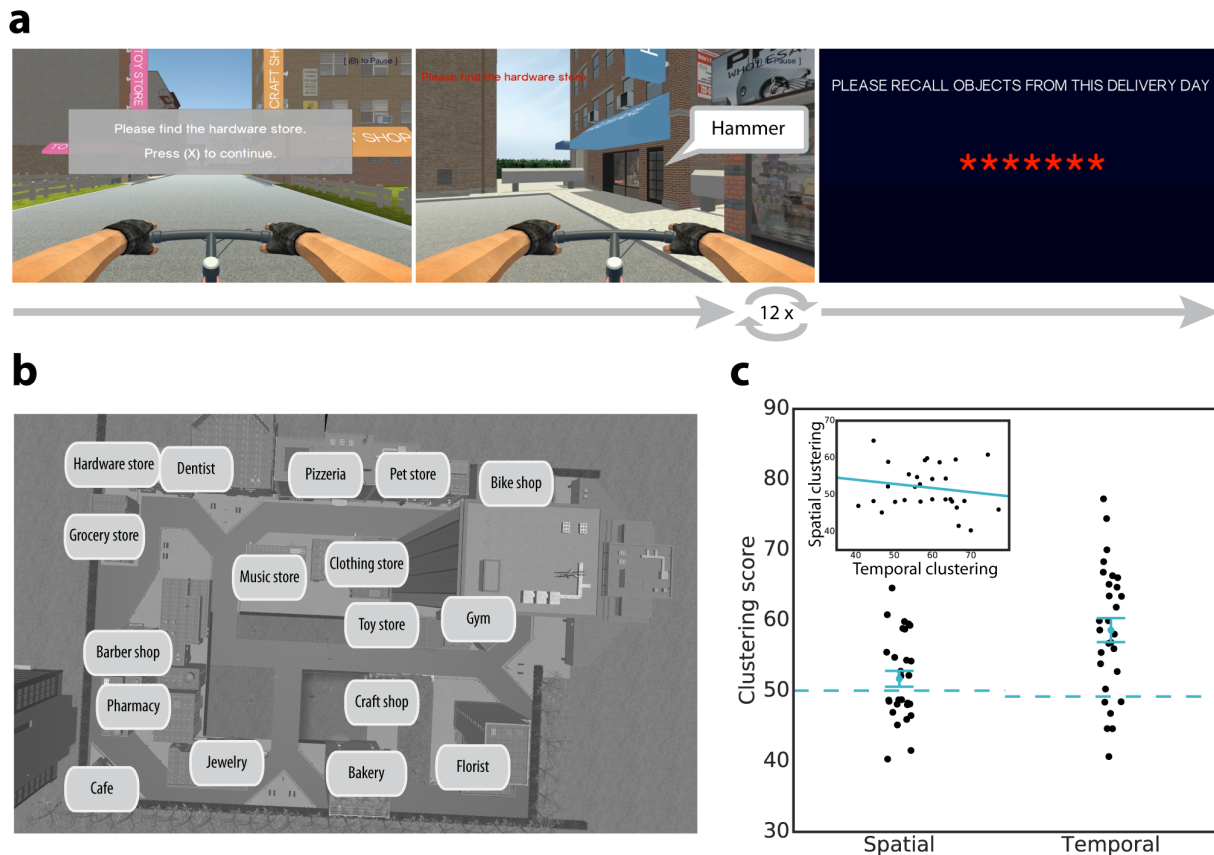
61 memory accuracy [16]. Together, these results suggest that low frequency oscillations orchestrate
62 place and grid cell firing and are part of a coding scheme for spatial information in the service of
63 orientation and navigation [21].

64 In the episodic memory domain, the HC and surrounding parahippocampal gyrus (PHG),
65 constitute the MTL memory system [22]: a system thought to form and retrieve event memories
66 by associating arbitrary stimulus combinations. Across different theories, there is consensus that
67 the PHG (including perirhinal, parahippocampal and entorhinal cortices) processes memory
68 attributes earlier and more distinctly than the HC [23–26]. Accordingly, the PHG separately
69 represents item and spatio-temporal context information [24,25]. The PHG projects to the HC,
70 where item information is integrated with spatio-temporal context information [23–25,27]. Despite
71 the striking anatomical overlap of spatial coding and episodic memory in the MTL, remarkably
72 little is known about potential shared neurophysiological mechanisms. Theta oscillations have
73 been suggested to support the formation of both spatial and episodic associations by organizing
74 spike-timing and associated plasticity [28], but evidence in favor of this idea is scarce. In fact,
75 successful episodic memory operations are often associated with a wide-spread decrease in low-
76 and increase in high-frequency power [29–32]. Despite such broad-band tilt effects, however, more
77 localized increases in temporal narrow-band theta oscillations during successful encoding [33] and
78 retrieval [30,31] also exist. These might more specifically relate to recollection of contextual
79 information [34,35].

80 Here, we use a hybrid spatial-episodic memory task in combination with intracranial
81 electroencephalography (iEEG) to assess the role of low- and high-frequency activity for episodic
82 retrieval of spatial context information in the MTL. In our task, subjects played the role of a
83 courier, riding a bicycle and delivering parcels to stores located within a virtual town (**Figure 1a-**
84 **b**). On each trial subjects navigate to a series of stores and subsequently are asked to recall all

85 objects they delivered. Based on the prominent role of theta oscillations for spatial memory and
 86 the idea that they specifically relate to contextual retrieval, we hypothesize that episodic retrieval
 87 of spatial context information, in contrast to more general biomarkers of successful memory, is
 88 accompanied by increased medial temporal theta power.

89



90 **Figure 1. Task design and behavioral clustering.** a) Hybrid spatial-episodic memory task in which subjects play the
 91 role of a courier. On each trial, subjects navigate to 12 different target stores to deliver parcels. Upon arrival at a target
 92 store, the just-delivered object is revealed. After 12 deliveries, subjects navigate to a final store. Here, the screen goes
 93 black and subjects attempt to freely recall all objects they delivered in any order. b) Bird's-eye view of the virtual city
 94 containing streets, target stores and non-target buildings. Subjects never saw this view. c) Clustering in recall
 95 sequences. Subjects organize their recalls with respect to spatial and temporal context information, as indicated by
 96 spatial and temporal clustering scores larger than 50 (higher scores are associated with closer recall transitions; for
 97 details see Methods). Error bars show the standard error of the mean (SEM). Dashed lines indicate the average of a
 98 permutation distribution. Spatial and temporal clustering are uncorrelated across subjects (inset).

99

100 We then turn from spectral biomarkers of spatial context retrieval to more specific
 101 reactivated spatial representations. Prior research has shown that place-responsive cells in the
 102 human MTL reinstate their activity during recall of words that were encoded in the part of the

103 environment corresponding to their place field [36]. The temporal dynamics of reinstatement in
104 different MTL sub-regions, however, remained unknown. To assess these dynamics, we use
105 representational similarity analyses in combination with a sliding window approach. Based on the
106 idea that information flow in the MTL reverses during retrieval [37], we propose that spatial
107 information is initially retrieved in the HC, and from there reinstates activity in PHG.

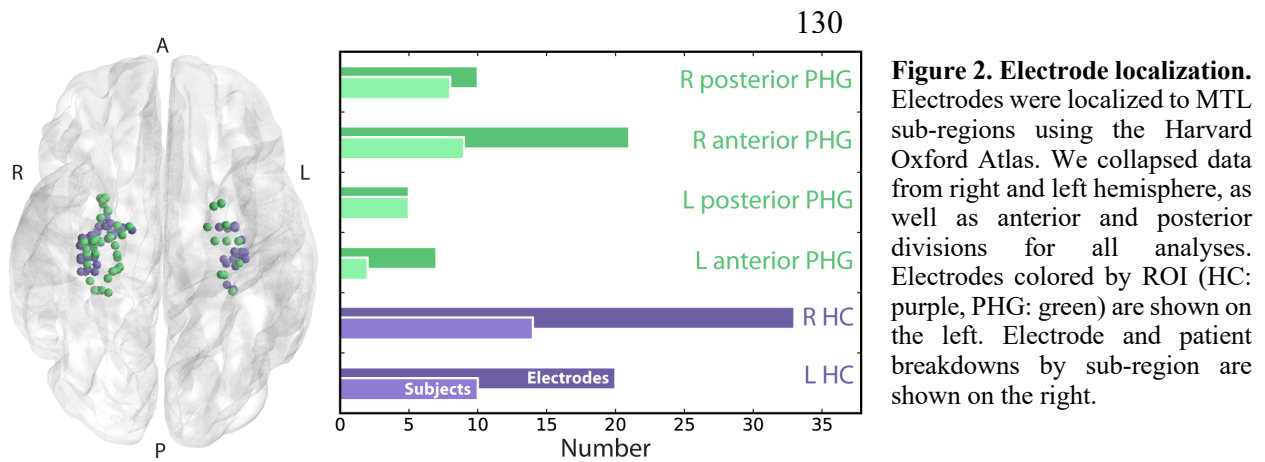
108 Finally, we ask how retrieved information is transferred between HC and PHG. Theta
109 oscillations have been strongly implicated in inter-regional connectivity during successful memory
110 operations [29,34,38,39] and in rodents place-responsive cells are locked to both theta and gamma
111 oscillations [40,41], suggesting that assemblies of neurons are organized by a theta-gamma code
112 [42,43]. Furthermore, reactivation of remembered stimuli has been shown to occur during
113 particular phases of the theta cycle [44,45]. Based on these findings, we suggest that theta and
114 gamma oscillations promote information transfer between HC and PHG during retrieval of
115 episodic information [29,46]. Specifically, we explore whether theta phase to gamma amplitude
116 coupling between HC and PHG increases during recall of spatial context to facilitate information
117 transfer from HC to PHG.

118

119 **Results**

120 Subjects recalled an average of 49.8% of words, while exhibiting both primacy (serial positions 1-
121 3 vs. 4-9; $t_{(28)} = 2.94$, $p = 0.007$, Cohen's $d = 0.16$) and recency (serial positions 10-12 vs. 4-9, $t_{(28)}$
122 $= 4.80$, $p < 0.001$, Cohen's $d = 0.89$) effects. They organized their recalls according to both
123 temporal ($p < 0.001$) and spatial ($p = 0.04$) encoding context, as determined by a permutation test
124 of their spatial and temporal clustering scores (**Figure 1c**; higher scores indicate stronger
125 spatial/temporal organization, see Methods for details). This means that subjects tended to

126 successively recall items, which were encoded at proximate serial positions or at proximate
127 locations in the virtual environment. Across subjects there was no correlation between spatial and
128 temporal clustering scores ($r_{(27)} = -0.15, p = 0.43$), suggesting that there is no subject-specific
129 variable such as associative memory performance or strategy use that drives these effects.



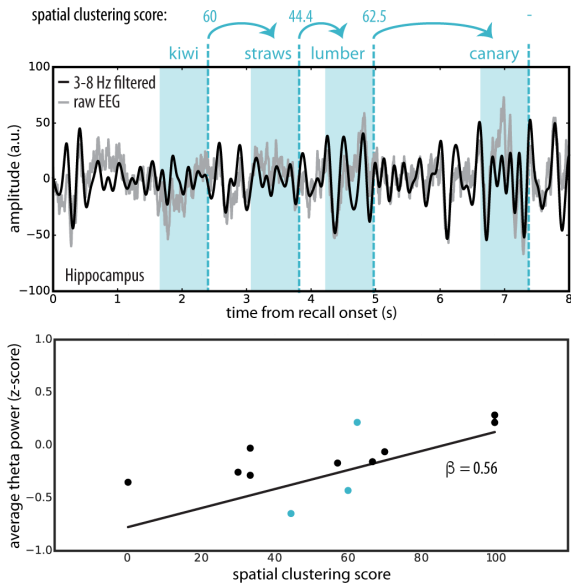
144
145 To identify the spectral signature of spatial context retrieval, we exploited the fact that
146 spatial clustering during recall is indicative of successful retrieval of spatial context information.
147 When spatial context is retrieved, along with an object's identity, it serves as a cue for other objects
148 encoded in a similar spatial context, and thereby favors spatially close recall transitions. With this
149 logic in mind, we assessed the role of theta and gamma activity in the HC and PHG (see **Figure 2**
150 for electrode locations) for spatial context retrieval using a within-subject linear regression model.
151 The model relates spectral power preceding vocal recall of each object to the spatial proximity
152 between the encoding locations of that object and the next recalled object (**Figure 3a**; see Methods
153 for details). A positive relation (i.e. β parameter) would indicate a power increase during retrieval
154 of spatial context, whereas a negative relation would indicate a power decrease.

a Encoding

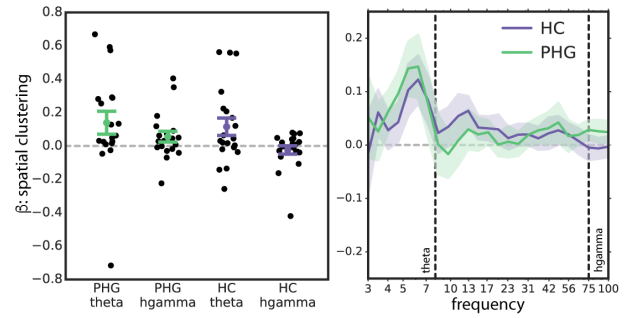
albums kiwi paint toothpaste shaving-cream canary roses rope amethyst baking-soda straws lumber



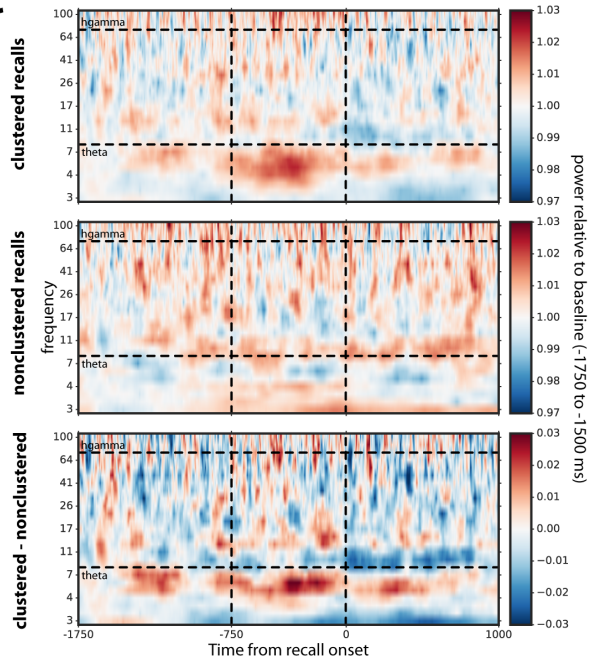
Retrieval



b



c



155 **Figure 3. The spectral signature of spatial context retrieval.** a) Sample encoding trial, in which 12 items were
 156 sequentially encoded in different locations of the virtual town (top). During recall, retrieved context cues items
 157 experienced in a similar encoding context. Retrieval of spatial context can therefore be inferred from the spatial
 158 proximity (i.e. clustering score) associated with each recall transition. The middle panel depicts an example trace of
 159 average hippocampal raw and theta-filtered EEG during recall (power was extracted from -750 to 0 ms prior to word
 160 onset; shaded regions) along with the spatial clustering scores for each transition. We collapsed data from all trials of
 161 a given subject and used linear regression to relate power prior to recall of each word to the spatial clustering score
 162 associated with transitioning to the next word (bottom). The three transitions illustrated in the hippocampal timeseries
 163 appear as blue dots in the scatter plot. A positive β indicates stronger power during retrieval of spatial context. b) β
 164 parameters (\pm SEM) for all subjects as a function of brain region and frequency band are shown on the left. Theta (3-
 165 8 Hz), but not high gamma (hgamma; 70-100 Hz), power increases in hippocampus (HC) and parahippocampal gyrus
 166 (PHG) during spatial context retrieval. β parameters (\pm SEM) across the entire frequency spectrum are shown on the
 167 right. Strongest increases in power were observed around \sim 5-7 Hz. c) Increases in theta power for spatially clustered
 168 (SCS > 70) compared to non-clustered recalls (SCS \leq 30) are also visually evident in raw power spectra averaged over
 169 HC and PHG for all subjects. The average power spectra per subject were baseline corrected with a relative baseline
 170 from -1750 to -1500 ms.

171

172

173 **Figure 3b** shows the β parameters for spatial proximity across all subjects. We found a
174 significant effect of frequency ($F_{(1,74)} = 5.57$, $p = 0.02$, $\eta_p^2 = 0.07$), with more positive β 's for theta
175 than high gamma power. Average β 's in the HC and PHG were also significantly larger than zero
176 for theta ($t_{(24)} = 2.29$, $p = 0.03$, Cohen's $d = 0.46$) but not gamma ($t_{(24)} = 0.96$, $p = 0.35$, Cohen's d
177 $= 0.19$) power. There was no effect of brain region ($F_{(1,74)} = 1.18$, $p = 0.28$, $\eta_p^2 = 0.016$) and no
178 interaction ($F_{(1,74)} = 0.34$, $p = 0.56$, $\eta_p^2 = 0.005$). The increase in theta power prior to spatially
179 clustered recalls in HC and PHG is also visually evident in the average raw time-frequency spectra
180 (**Figure 3c**). These results suggest that retrieval of spatial information during episodic free recall
181 and associated clustering of recall sequences is associated with increased theta power in the HC
182 and PHG.

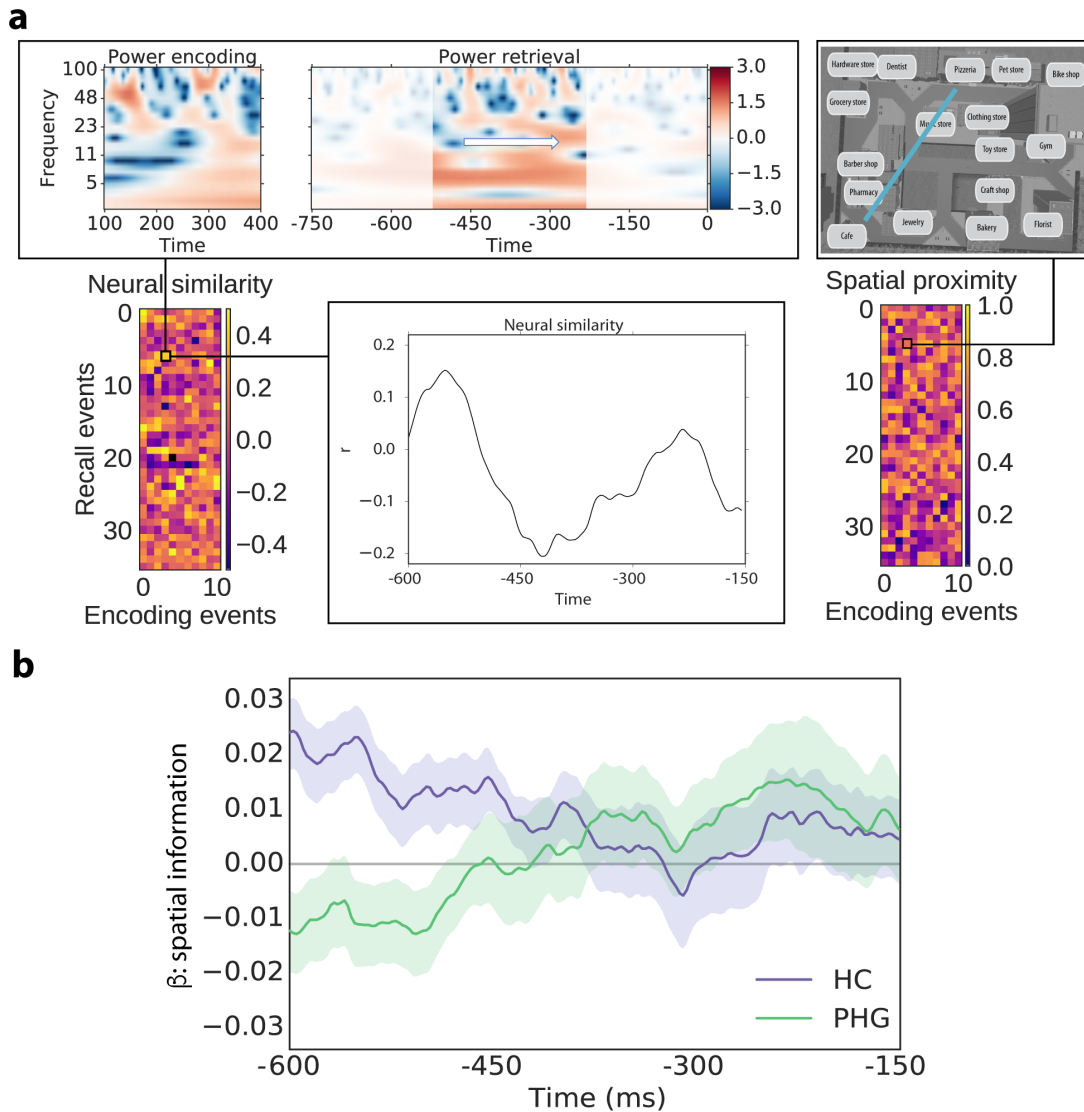
183 We performed a parallel exploratory analysis to establish whether a similar increase in
184 theta power occurs for transitions that are temporally, rather than spatially, close. Average β 's
185 relating temporal clustering scores to theta power in the HC and PHG were not significantly
186 different from zero ($t_{(24)} = 0.16$, $p = 0.88$, Cohen's $d = 0.03$). Furthermore, in direct comparison,
187 the average increase in theta in PHG and HC during spatially close transitions was marginally
188 stronger than that during temporally close transitions ($t_{(24)} = 2.02$, $p = 0.055$, Cohen's $d = 0.40$),
189 tentatively suggesting that the observed effect might be specific to or stronger during recall of
190 spatial compared to temporal context information.

191 Next, we sought to assess dynamic reinstatement of specific spatial representations in HC
192 and PHG. To this end, we used encoding-retrieval similarity analyses with a sliding window
193 approach. Specifically, we correlated a vector representing power during encoding for all
194 electrodes in HC or PHG, all frequencies and time-points with a corresponding retrieval vector
195 derived from a sliding time-window to track reactivation (i.e. neural similarity) of encoding
196 features leading up to recall (**Figure 4a**). Applying a rationale similar to the one described above,

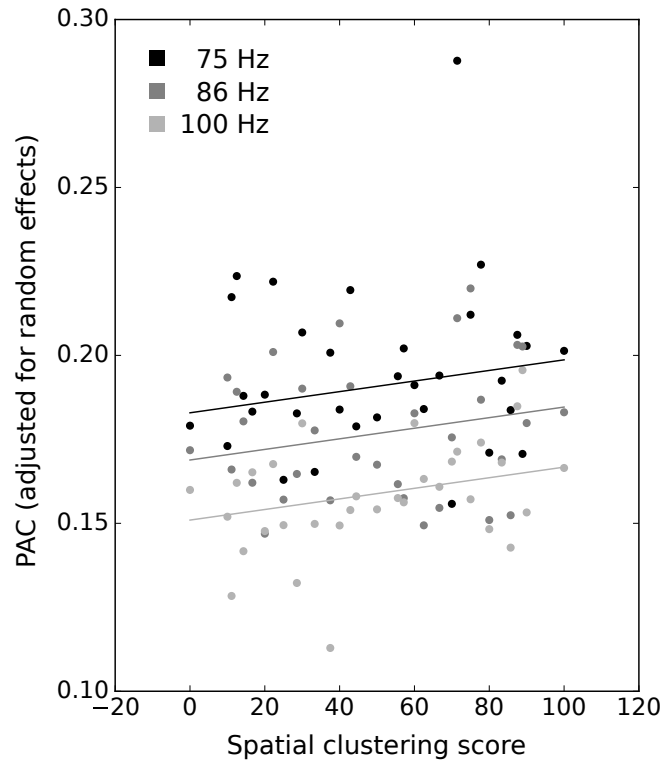
197 we used the spatial proximity between the locations associated with each encoding and recall event
198 pair to isolate representations of spatial context. The degree to which similarity of encoding and
199 recall events can be explained by the proximity between their associated encoding locations
200 provides an estimate of the amount of reactivation of spatial context information during recall. We
201 estimated this relation in a within-subjects approach separately for each time-point leading up to
202 recall using linear regression of neural similarity and spatial proximity (see Methods for details).
203 At each time-point, a β value above 0 indicates higher similarity for encoding-recall pairs that
204 share spatial context and, hence, can be interpreted as the instantaneous amount of reactivated
205 spatial information. To exclude confounding this measure with reinstatement of item-level
206 information, we excluded encoding-recall pairs of the same item.

207 We observed distinct temporal profiles of spatial context reinstatement in the HC and PHG:
208 Whereas our index of retrieved spatial information numerically decreased in the HC, it increased
209 in the PHG leading up to recall (**Figure 4b**). To quantify this difference in temporal trend, we used
210 a linear mixed effects model (see Methods for details). Using likelihood ratio tests, we observed a
211 main effect of brain region ($\chi^2_{(1)} = 83.93$, $p < 0.001$) with stronger spatial reactivation in HC than
212 PHG, as well as a main effect of time ($\chi^2_{(1)} = 15.18$, $p < 0.001$) with stronger spatial reactivation
213 at early time points. We also observed a region by time interaction ($\chi^2_{(1)} = 293.32$, $p < 0.001$),
214 indicating different time courses of reactivation in HC and PHG. Reducing the model to a single
215 brain region, revealed a negative effect of time in the HC (i.e. spatial information decreased; $\chi^2_{(1)}$
216 $= 181.69$, $p < 0.001$) and a positive effect of time in the PHG (i.e. spatial information increased;
217 $\chi^2_{(1)} = 300.15$, $p < 0.001$). Removing all fixed effects in the model revealed a trend-level significant
218 intercept ($z = 1.69$, $p = 0.091$), which can be interpreted as the overall degree of spatial reactivation
219 irrespective of brain region and timing. These results indicate that spatial context is reactivated

220 with distinct time courses in HC and PHG. Specifically, they support the notion that spatial
 221 information is initially retrieved in the HC and then relayed to cortical modules in the PHG.



222 **Figure 4. Reinstatement of spatial information leading up to recall.** a) To obtain an index of retrieved spatial
 223 information over time, we first calculated neural encoding-retrieval similarity for a 300 ms encoding time window
 224 and a sliding 300 ms retrieval time window centered between -600 and -150 ms (i.e. half a window size from the edges
 225 of each retrieval epoch). We thereby obtained a measure of neural similarity (i.e. reactivation) over time for each
 226 encoding-recall event pair for each subject. Since we were specifically interested in reactivation of spatial information,
 227 we then used a within-subject regression model to relate neural encoding-retrieval similarity at each time point to
 228 the spatial proximity between the locations associated with the respective encoding and recall events. b) The average
 229 resulting β parameters across subjects (\pm SEM) are plotted as function of time, separately for hippocampus (HC) and
 230 parahippocampal gyrus (PHG). A β parameter above 0 indicates higher similarity for encoding-recall pairs that share
 231 spatial context and, hence, can be interpreted as reactivated spatial information. Spatial information is represented
 232 more strongly in HC at the beginning of the epoch. Subsequently, information decreases in HC and increases in PHG
 233 leading up to recall.



234 **Figure 5. Theta-phase to gamma-amplitude coupling between hippocampus (HC) and parahippocampal gyrus**
 235 **(PHG).** Average indices of the strength of phase amplitude coupling (PAC; Fisher z-transformed and adjusted for
 236 random effects in our model) across subjects for each gamma frequency as a function of spatial clustering scores.
 237 Using the same rationale as in the analysis displayed in Figure 3, we used a regression model to relate PAC to spatial
 238 clustering scores, which in turn serve as a proxy for spatial context retrieval. PAC was higher during retrieval of spatial
 239 context (i.e. for spatially close recall transitions) in a broad high-frequency band.

240

241 Finally, we explored theta-gamma phase-amplitude coupling between these two brain

242 regions (i.e. a modulation of parahippocampal gamma amplitude by hippocampal theta phase) as

243 a mechanism of information transfer. To this end we calculated the synchronization index (SI) [47]

244 between hippocampal theta phase and the phase of the parahippocampal gamma power envelope

245 for all HC-PHG electrode pairs during recall. We then used a linear mixed effects model to relate

246 phase amplitude coupling (PAC; i.e. the magnitude of the SI) to spatial clustering scores across

247 recall events (see Methods for details). A positive relation would indicate that retrieval of spatial

248 context is associated with increased theta-gamma coupling between HC and PHG. Spatial

249 clustering was a significant positive predictor of PAC, as indicated by a likelihood ratio test

250 (Figure 5; $\chi^2_{(1)} = 23.01$, $p < 0.001$). This means that close spatial recall transitions (i.e. retrieval of
251 spatial context) were associated with an increase in theta-gamma coupling between HC and PHG.
252 We did not observe the same effect in the opposite direction (i.e. parahippocampal theta phase
253 modulating hippocampal gamma amplitude during close transitions; $\chi^2_{(1)} = 0.76$, $p = 0.383$) and
254 there was no effect of temporal clustering on PAC ($\chi^2_{(1)} = 0.57$, $p = 0.448$). We did observe a
255 negative main effect of frequency ($\chi^2_{(1)} = 143.61$, $p < 0.001$), with stronger PAC at lower gamma
256 frequency, but no interaction of spatial clustering and frequency. These results suggest that spatial
257 retrieval is linked to PAC between hippocampal theta and parahippocampal gamma in a broad
258 high frequency range, implicating PAC in transfer and coding of spatial information in the MTL.

259

260 Discussion

261 Episodic memory refers to our ability to associate events with a specific spatio-temporal
262 context. Whereas numerous studies have long implicated temporal context as a powerful
263 organizing principle in episodic retrieval [1,2], the organization of episodic memories by spatial
264 context has only recently received attention [3,48]. Our behavioral results demonstrate that when
265 a spatial study context is made available by use of a virtual environment, subjects are more likely
266 to recall items in succession that were encoded at proximate spatial locations. This spatial
267 contiguity effect mirrors the well-established temporal contiguity effect in which subjects also tend
268 to successively recall items studied in temporally proximate positions within a list. We thus find
269 that like temporal context, spatial context also appears to reinstate during episodic memory
270 retrieval.

271 To help elucidate the physiological basis of spatial-context reinstatement, we related the
272 spatial proximity associated with each recall transition (a measure of spatial-context reinstatement)

273 to spectral power during retrieval. We observed increased medial temporal theta, but not gamma
274 power, to co-occur with retrieval of spatial context and associated clustering. This finding is in
275 line with studies linking theta power to recollection of contextual information [34,35], as well as
276 with a study showing that theta power in the HC increases during retrieval of items that were
277 encoded in semantically structured lists [31]. They thereby specifically indicate a role for theta
278 oscillations in retrieving items that are accompanied, organized and cued by their encoding
279 context. Our results might initially seem at odds with studies observing a spectral tilt with increased
280 high-frequency power and decreased low-frequency power leading up to successful recall
281 compared to deliberation [29–32]. At a closer look, they seem to indicate that a more strongly
282 matched recall contrast (such as recall with vs. without contextual information) reveals a neural
283 signature of associative retrieval that is often hidden under a global spectral tilt, which may, in
284 turn, relate to more general activation/attention processes accompanying recall. The current results
285 furthermore tentatively point to an even more specific role of theta in retrieving spatial (as opposed
286 to other types of) context information, given that we did not observe a similar increase in theta
287 power for temporally close recall transitions (although see Solomon et al. (2019) for a more in-
288 depth analysis of theta power and temporal distance).

289 This finding is of particular interest, given the known role of theta oscillations in navigation
290 and spatial memory [50]. Theta oscillations have been observed in the rodent [8,9] and human
291 [11,12,14,15] MTL during movement compared to stillness. In rodents, they have been linked to
292 the spiking of place responsive cells [17–19]. In humans, theta power in the MTL has been
293 implicated in coding spatial distances during and preceding navigation [12] or during teleportation
294 [51], suggesting that spatial distances are coded in theta even in the absence of sensory cues. In a
295 cued location memory task, theta power has further been shown to be indicative of successful
296 encoding of spatial locations [52]. And using MEG, theta power has been related to trajectory

297 changes, cued retrieval of spatial locations and navigation performance [10,13,53]. Taken together
298 these findings implicate theta in the encoding, retrieval and online-maintenance of spatial locations
299 that underlie spatial orientation and navigation. Notably, in our task, the increase in theta power
300 we observed occurred in the absence of any affordances to maintain or recall spatial information,
301 while subjects viewed a black screen. Our results therefore extend previous findings to suggest
302 that theta oscillations provide a common electrophysiological signature of spatial coding during
303 navigation, explicit spatial memory demands and incidental episodic retrieval of spatial context
304 information.

305 But where, when and how exactly is spatial information retrieved? It has previously been
306 shown that place-responsive cells in the human MTL reinstate their spiking activity during recall
307 of items encoded within a cell's place field [36]. It remained unknown, however, what the temporal
308 dynamics of reinstatement in different MTL sub-regions are and how information is routed
309 between them. The results of our encoding-retrieval similarity analysis suggest that spatial
310 information is reinstated with distinct temporal profiles in HC and PHG. Whereas spatial
311 information is reinstated early in HC, information in PHG builds up closer to recall. This pattern
312 of results suggests that initial retrieval of spatial information occurs in the HC and, from there, is
313 relayed to the PHG. It thereby supports theories claiming that the primary direction of information
314 flow during retrieval is from HC to the neocortex [37] and is in line with two studies on cued recall
315 of object-scene pairs: Using fMRI, Staresina and colleagues (2013) observed differential onset
316 latencies in category-selective regions of the PHG specialized for objects and scenes, depending
317 on which type of information served as object and which as cue. Dynamic causal modeling
318 analyses in the same data set favored a model in which information was routed from PHG via HC
319 back to PHG [54]. The second study used single-unit recordings from HC and entorhinal cortex to
320 show that object reinstatement in EC is linked to changes in firing rate in the HC during successful

321 associative retrieval and that HC spiking temporally precedes spiking in the entorhinal cortex [55].
322 Taken together these findings suggest that the HC is the initial locus of retrieval for associations
323 between item and spatial context (or objects and scenes) and that this information is relayed to
324 cortical regions in the PHG.

325 Alternatively, early reactivation in HC and later reactivation in PHG could be explained by
326 a third source projecting to both brain-regions with distinct time delays. We cannot rule out this
327 alternative explanation in the current data set but suggest that future studies could clarify the degree
328 to which early reactivation in HC is causally related to later reactivation in PHG using direct
329 electrical stimulation. If disruptive stimulation in HC during an early time-window, but not in a
330 late time-window, disrupts reactivation in PHG, this would provide further evidence for direct
331 information-transfer between these regions.

332 Future research could help elucidate the nature of neural representations being reinstated
333 in the HC or PHG. Spatially responsive cells have different tuning properties in different sub-
334 regions of the MTL. In the rat, place cells with the most distinct firing fields are found in the CA
335 areas of the HC, whereas grid cells are found in the entorhinal cortex [56]. Evidence in humans is
336 scarce but seems to be broadly consistent with this [4,6,57]. In humans, a different type of cells
337 located in the PHG responds to view of specific landmarks, irrespective of a subjects' location [4],
338 suggesting that these cells are more sensitive to visual features than abstract location. Based on
339 these and other considerations [24,25], one can expect that the type of spatial representation that
340 is reinstated, as well as its link to other types of episodic content, differs between different regions
341 in the MTL, potentially with an abstract to concrete gradient from HC, over entorhinal cortex, to
342 PHG. Whereas our analyses of spatial context reinstatement assumed a linear relation between
343 actual and representation spatial distance (i.e. **Figure 4** shows the linear relation between neural
344 similarity and spatial proximity over time), it is possible that some regions of the MTL do not

345 represent spatial information on such a linear scale: A region that primarily cares about visual
346 features of scenes, for instance, might exhibit strong neural similarity at all locations providing a
347 similar view and low similarity otherwise. More research is needed to understand reactivation of
348 such spatial features that are non-linearly related to spatial distance.

349 Having established differential timing of spatial reactivation in HC and PHG, we next
350 asked whether phase-amplitude coupling might serve as a mechanism of information transfer
351 between these regions. Indeed, our analyses revealed that theta-phase to gamma-amplitude
352 coupling between HC and PHG increases during retrieval of spatial (but not temporal) context in
353 a broad high-frequency range. Prior studies in humans have implicated local theta-gamma coupling
354 within the HC as well as coupling between frontal and posterior regions in scalp EEG to successful
355 memory encoding and recognition [58–60]. In rats, coupling in CA regions of the HC was
356 associated with successful retrieval [61,62]. Our results demonstrate, that theta-gamma coupling
357 in humans specifically supports retrieval of spatial context. They further indicate that hippocampal
358 theta is coupled to gamma oscillations outside the HC proper (i.e. in the PHG) during memory
359 retrieval, and hence might be involved in inter-regional communication and information transfer.

360 Although we have interpreted our findings as demonstrating the reinstatement of spatial
361 information during the recall phase, it is also possible that spatial clustering arises due to the
362 reactivation of object representations during encoding. Specifically, if subjects reactivate object
363 representations whenever they visit locations close to an object’s initial encoding location, this
364 would establish temporal associations between objects encoded in proximate locations – spatial
365 context would become an integral part of temporal context. In the recall phase, temporal context
366 would then be sufficient to cue items from a proximate location. We believe that this process might
367 enhance the observed effects, but it seems unlikely to explain them entirely, as it would mean that
368 spatial context reliably cues items during encoding but completely fails to do so during recall.

369 To summarize, we show that episodic memories are organized by spatial study context,
370 resulting in a spatial contiguity effect that parallels the often-reported temporal contiguity effect
371 in free recall. We further demonstrate that increased medial temporal theta power accompanies
372 retrieval of spatial context and associated clustering behavior, implicating theta oscillations as a
373 common neurophysiological substrate of spatial coding in navigation and episodic retrieval.
374 Exploring the temporal dynamics of reinstatement in HC and PHG, we find that spatial context
375 information is initially retrieved in the HC and emerges later in the PHG. Finally, we demonstrate
376 that hippocampal theta phase modulates parahippocampal gamma amplitude during retrieval of
377 spatial context, suggesting a role for cross frequency coupling in coding and transmitting retrieved
378 information.

379 **Methods**

380 **Participants**

381 29 patients with medication-resistant epilepsy undergoing clinical seizure monitoring at
382 Thomas Jefferson University Hospital (Philadelphia, PA, USA), the University Clinic Freiburg
383 (Freiburg, GER) and the Hospital of the University of Pennsylvania (Philadelphia, PA, USA)
384 participated in the study. The study protocol was approved by the Institutional Review Board at
385 each hospital and subjects gave written informed consent. Electrophysiological data were recorded
386 from depth electrodes placed, according to clinical considerations, in the HC and/or surrounding
387 PHG.

388

389 **Experimental design and task**

390 Subjects played the role of a courier in a hybrid spatial-episodic memory task, riding a
391 bicycle and delivering parcels to stores located within a virtual town (consisting of roads, stores,

392 task-irrelevant buildings, areas of grass, and props such as fences, streetlights and trees; **Figure 1a-**
393 **b).** Each experimental session consisted of a series of delivery days (i.e. trials), during which
394 subjects navigate to deliver objects and, at the end of each trial, recall those objects. Subjects
395 completed slightly different versions of this paradigm, the details of which are described in the
396 following paragraphs. These versions were programmed and displayed to subjects using the Panda
397 Experiment Programming Library [63], which is a Python based wrapper around the open source
398 game engine Panda3d (with 3D models created using Autodesk Maya™) or the Unity Game
399 Engine (Unity Technologies, San Francisco, CA).

400 Prior to starting the first delivery day, subjects viewed a static or rotating rendering of each
401 store in front of a black background. Each store had a unique storefront and a sign that
402 distinguished it from task-irrelevant buildings. This ‘store familiarization’ phase was followed by
403 a ‘town familiarization’ phase, in which subjects were instructed to navigate from store to store
404 without delivering parcels (and recalling objects), visiting each store 1-3 times in pseudo-random
405 order (each store was visited once, before the first store was visited the second time). Subjects
406 were informed about their upcoming goal by on-screen instructions and navigated using the
407 joystick or buttons on a game pad. Location-store mappings in the town were fixed for 7 subjects
408 and random for 22 subjects (the layout was always fixed across experimental sessions; i.e. each
409 subject experienced the same town layout across sessions). For a subset of the subjects, the town
410 and store familiarization phases were part not only of the first but also all following sessions with
411 just one visit to each store prior to the first delivery day in each session. Furthermore, waypoints
412 helped a subset of subjects navigate upon difficulties finding a store. Considering each intersection
413 as a decision point, arrows pointing in the direction of the target store appeared on the street after
414 three bad decisions (i.e. decisions that increased the distance to the target store).

415 Each delivery day trial consisted of a navigation phase and a free recall phase (and for some
416 subjects an additional cued recall phase following free recall, for which no data is reported here;
417 **Figure 1a**). For the navigation phase, 13 stores were chosen at random out of the total number of
418 16 or 17 stores. Subjects navigated to these stores sequentially (including on-screen instructions
419 and waypoints described above). Upon arrival at the first 12 stores, subjects were presented with
420 an audio of a voice naming the object (N = 23 subjects; variable duration on the order of 1-2 s) or
421 an image of the object (N = 6 subjects; 5 s) they just delivered. For 15 subjects, objects were drawn
422 with and for 14 subjects without replacement. For 23 subjects, objects were semantically related
423 to their target store to aid recall performance. Object presentation was followed by the next on-
424 screen navigation instruction (“Please find store X”). Upon arrival at the final store, where no item
425 was presented, the screen went black and subjects heard a beep tone. After the beep, they had 90
426 s to recall as many objects as they could remember in any order. Vocal responses were recorded
427 and annotated offline. Subjects completed a variable number of delivery days per session (min: 2,
428 max: 14, mean = 6). A final free recall phase followed on the last delivery day within each session,
429 for which no data is reported here.

430

431 **Behavioral analyses of recall transitions**

432 Behavioral data were analyzed using Python version 2.7. To assess organization of recall
433 sequences by retrieved spatial (and temporal) context, we assigned each recall transition the
434 Euclidean (temporal) distance between the two encoding locations (time points). In the same way,
435 we calculated the distance for all possible transitions that could have been made instead of each
436 actual transition (i.e. the distance between the location (time point) of the first item in the transition
437 and all locations (time points) at which objects were encoded that had not yet been recalled at a
438 given recall transition). We then calculated a spatial (temporal) clustering score for each recall

439 transition as 100 minus the percentile ranking of the spatial (temporal) distance assigned to the
440 actual transition with respect to all possible transitions. The higher the average spatial (temporal)
441 clustering score across recall transitions, the more likely a subject was to transition between items
442 that were encoded at proximate locations (time points). We used a permutation procedure to assess
443 significance of spatial (temporal) clustering across subjects. To do so, all recalled words on a given
444 trial for a given subject were randomly permuted 2000 times. The distribution of average clustering
445 scores across subjects obtained from these random permutations provides a measure of clustering
446 values observed by chance, while controlling for the identity and number of recalled words per
447 trial. The percentage of random clustering scores larger than the observed clustering score
448 constitutes the permutation p-value. To assess the relation between spatial and temporal clustering,
449 we computed the correlation between both variables across subjects.

450

451 **Intracranial EEG data acquisition and preprocessing**

452 EEG data were acquired using AdTech (Oak Creek, WI, USA), PMT (Chanhasen, MN,
453 USA) or Dixi (Besançon, France) depth electrodes along with a Nihon Koden (Tokyo, Japan),
454 Natus (Pleasanton, CA, USA), Compumedics (Abbotsford, Victoria, Australia) or IT-med
455 (Usingen, Germany) recording system at sampling rates between 400 and 2500 Hz. Coordinates
456 of the radiodense electrode contacts were derived from a post-implant CT or MRI scan and then
457 registered with the pre-implant MRI scan in MNI space using SPM or Advanced Normalization
458 Tools (ANTS)[64]. EEG data were analyzed using Python version 2.7 along with the Python Time
459 Series Analyses (pts; https://github.com/pennmem/pts_new) and MNE [65] software packages.
460 EEG data were aligned with behavioral data via pulses send from the behavioral testing laptop to
461 the EEG system. Data were epoched from -1900 ms to 2400 ms with respect to word onset during
462 encoding and from -2750 ms to 2000 ms with respect to recall onset during retrieval periods. Data

463 were re-referenced with a bipolar reference scheme and down-sampled to 400 Hz. A butterworth
464 filter (order 4; cutoff frequencies 48 to 52 for data recorded in Germany and 58 to 62 for data
465 recorded in the US) was used to filter line noise and subsequently outliers were excluded on an
466 epoch by channel basis: The interquartile range (IQR) was calculated for each channel across all
467 (mean-corrected) encoding or retrieval events within a session. Outliers were identified as samples
468 5 times the IQR above the 75th percentile or 5 times the IQR below the 25th percentile. Epochs
469 were excluded for a given channel with at least one outlying sample. On average 2.5 % (min: 0 %,
470 max 11.0 %) of epoch-channel pairs were excluded per session. To extract power and phase, the
471 data were convolved with complex Morlet wavelets (5 cycles) for 25 log-spaced frequencies
472 between 3 and 100 Hz. After convolution, a buffer was removed at the beginning and end of each
473 epoch leaving a time window of 100 ms to 400 ms during encoding and -750 ms to 0 ms during
474 recall. Data were z-scored with respect to the mean and standard deviation across all encoding or
475 recall samples within a session and, depending on the analysis, averaged over time, two frequency
476 bands (theta: 3 to 8 Hz; high gamma: 70 to 100 Hz), and two regions of interest (ROI): HC and
477 PHG as defined by the Harvard Oxford Atlas. Subjects' data were included for a given analysis if
478 they contributed at least 8 valid trials in at least one (or, where necessary, both) ROI(s).

479

480 **Intracranial EEG data statistical analyses**

481 To assess the spectral correlates of successful spatial context retrieval and associated
482 spatial clustering, we used a within-subject linear regression model. The model relates average
483 theta and high gamma power in the HC (N = 20 subjects) and PHG (N = 19 subjects) preceding
484 recall of the first item in a recall transition to the spatial proximity (i.e. spatial clustering score)
485 associated with that transition. To the extent that retrieved spatial context cues items encoded in
486 close spatial proximity, the spatial proximity of a recall transition should be indicative of spatial

487 context retrieval for the first item in the transition. A β value for spatial proximity above zero
488 indicates increased power during retrieval of spatial context, and a value below zero indicates
489 decreased power during retrieval of spatial context. In addition to the spatial clustering score
490 associated with each recall transition, temporal clustering score, serial position and output position
491 were added as regressors of no interest to account for shared variance with our predictor of interest.
492 The β values for spatial clustering scores per region and frequency band for all subjects were
493 analyzed with a 2x2 ANOVA and a two-sided one-sample t-test.

494 To test for dynamic spatial context reinstatement, time-frequency spectra (25 log-spaced
495 frequencies between 3 and 100 Hz) during encoding and retrieval were concatenated over all
496 electrodes within either HC (N = 20 subjects) or PHG (N = 20 subjects). A single vector
497 representing power for all time-frequency-electrode points within a given ROI during encoding
498 was correlated with a corresponding vector for retrieval derived from a sliding time-window. The
499 sliding time-window equaled the length of the encoding epoch (300 ms) and was centered on every
500 sample (every 2.5 ms) in the retrieval time-window (-750 ms to 0 ms), located at least half a
501 window size (150 ms) from the edges of the retrieval time-window. For each recall event, we
502 calculated the correlation (i.e. neural similarity) with all encoding events on the same list that did
503 not share the same item. We excluded encoding of the respective item to exclude effects driven by
504 reinstatement of item as opposed to context information. We then used a linear regression model
505 relating (Fisher z-transformed) neural similarity at each time point to the spatial proximity
506 (normalized to be between 0 and 1) between the locations of the encoded and recalled item. A β
507 value above 0 indicates higher similarity for encoding-recall pairs that share spatial context and,
508 hence, can be interpreted as reactivated spatial context. Again, we included additional regressors
509 of no interest to account for shared variance: temporal proximity (the negative absolute temporal
510 difference between the two encoding time points) and study-test proximity (the temporal

511 difference between encoding and recall time). To quantify the temporal dynamics of reactivated
512 spatial information in HC and PHG, we used a linear mixed effects model with brain region, time
513 and their interaction as fixed effects and subject as a random intercept effect. Significance of fixed
514 effects was evaluated using likelihood ratio tests between a full model (both main effects or both
515 main effects and their interaction) and a reduced model (one or two main effects) with the effect
516 of interest removed.

517 To assess theta-phase to gamma-amplitude coupling between HC and PHG (N = 14
518 subjects), we calculated the SI [47]. This method does not require an a priori assumption about the
519 modulating (low) frequency, but instead this frequency is determined by finding a peak in the
520 power spectrum of the high frequency power envelope. If high frequency power is time-locked to
521 low frequency phase, high frequency power should fluctuate at the lower oscillation frequency. In
522 our analysis we restricted the range of modulating frequencies to the theta band (i.e. 3 to 8 Hz).
523 After determining the modulating frequency for each channel in the PHG, each recall event, and
524 each extracted frequency in the gamma band, we extracted the phase of the high frequency power
525 time series using the Hilbert transform. The SI is then calculated as the consistency across time
526 between the phase of the high frequency power time series (in PHG) and the low frequency filtered
527 signal (in HC) [47]. We excluded from this calculation 4 out of 96 available electrode pairs because
528 they shared a bipolar reference contact and PAC could therefore not clearly be attributed to a
529 between-region effect but could also stem from PAC within HC or PHG. The magnitude of the
530 resulting complex number indicates the extent of synchronization and the angle indicates the
531 preferred phase offset. We then asked if PAC (i.e. the magnitude of the SI) between HC and PHG
532 is a function of spatial clustering. To this end, we used linear mixed effects models to relate (Fisher
533 z-transformed) PAC to spatial clustering scores across recall events. We included electrode pair
534 nested in subject as random intercept effects, as well as spatial clustering score and modulated

535 gamma frequency (70-100 Hz) as fixed effects. In addition, power in the modulating theta
536 frequency (3-8 Hz) band was included as a fixed effect to control for the fact that PAC may be
537 confounded by differences in the reliability of phase estimation in time-windows of low vs high
538 power. Again, temporal clustering, serial position and output position were also included as
539 regressors of no primary interest to account for shared variance. Significance of fixed effects was
540 determined using likelihood ratio tests between a full model against a model without the effect in
541 question.

542

543 **Data availability**

544 The full dataset that supports the findings of this study is not publicly available due to it
545 containing information that could compromise research participant privacy/consent. Subsets of the
546 data will be available at http://memory.psych.upenn.edu/Electrophysiological_Data.

547

548 **Acknowledgements**

549 This work was supported by NIH grant MH061975 to MJK and by DFG grant HE 8302/1-
550 1 to NAH. We thank Christoph Weidemann for help with data analyses, Paul Wanda, Alison Xu,
551 Zeinab Helili, Katherine Hurley, Deb Levy, Logan O’Sullivan, Ada Aka and Allison Kadel for
552 help with data acquisition and post-processing, Jonathan Miller and Ansh Johri for their
553 contributions to the task design, Corey Novich and Ansh Patel for programming the Unity based
554 experiment, as well as Joel Stein, Rick Gorniak and Sandy Das for electrode localization support.
555 We are most grateful to all patients and their families who selflessly volunteered their time to
556 participate in this research.

557

558 **Author contributions**

559 NAH and MJK designed research, NAH analyzed data and drafted the paper, NAH and
560 MJK edited the paper, AB and NAH collected data, AS-B, MRS, ADS recruited participants and
561 performed clinical duties associated with data collection including neurosurgical procedures or
562 patient monitoring, MJK supervised research, all authors approved the final version of the paper.

563

564 **References**

565 1. Kahana MJ. Associative retrieval processes in free recall. *Mem Cognit.* 1996;24: 103–109.
566 doi:10.3758/BF03197276

567 2. Sederberg PB, Howard MW, Kahana MJ. A context-based theory of recency and contiguity
568 in free recall. 2009;115: 893–912. doi:10.1037/a0013396.A

569 3. Miller JF, Lazarus EM, Polyn SM, Kahana MJ. Spatial clustering during memory search. *J*
570 *Exp Psychol Learn Mem Cogn.* 2013;39: 773–781. doi:10.1037/a0029684

571 4. Ekstrom AD, Kahana MJ, Caplan JB, Fields TA, Isham EA, Newman EL, et al. Cellular
572 networks underlying human spatial navigation. *Nature.* 2003;425: 184–187.
573 doi:10.1038/nature01955.1.

574 5. O’Keefe J. A review of the hippocampal place cells. *Prog Neurobiol.* 1979;13: 419–439.

575 6. Jacobs J, Weidemann CT, Miller JF, Solway A, Burke JF, Wei X, et al. Direct recordings
576 of grid-like neuronal activity in human spatial navigation. *Nat Neurosci.* 2013;16: 1188–
577 1191. doi:10.1038/nn.3466

578 7. Hafting T, Fyhn M, Molden S, Moser M-B, Moser EI. Microstructure of a spatial map in
579 the entorhinal cortex. *Nature.* 2005;436: 801–806. doi:10.1038/nature03721

580 8. Buzsáki G, Leung L-WS, Vanderwolf CH. Cellular Bases of Hippocampal EEG in the
581 Behaving Rat. *Brain Res Rev.* 1983;6: 139–171.

582 9. Vanderwolf CH. Hippocampal electrical activity and voluntary movement in the rat.
583 *Electroencephalogr Clin Neurophysiol.* 1969;26: 407–418.

584 10. Cornwell BR, Johnson LL, Holroyd T, Carver FW, Grillon C. Human Hippocampal and
585 Parahippocampal Theta during Goal-Directed Spatial Navigation Predicts Performance on
586 a Virtual Morris Water Maze. *J Neurosci.* 2008;28: 5983–5990.
587 doi:10.1523/JNEUROSCI.5001-07.2008

588 11. Bohbot VD, Copara MS, Gotman J, Ekstrom AD. Low-frequency theta oscillations in the
589 human hippocampus during real-world and virtual navigation. *Nat Commun.* 2017;8: 1–7.
590 doi:10.1038/ncomms14415

591 12. Bush D, Bisby JA, Bird CM, Gollwitzer S, Rodionov R, Diehl B, et al. Human hippocampal
592 theta power indicates movement onset and distance travelled. *Proc Natl Acad Sci.* 2017;114:
593 12297–12302. doi:10.1073/pnas.1708716114

594 13. Kaplan R, Doeller CF, Barnes GR, Litvak V, Duezel E, Bandettini PA, et al. Movement-
595 Related Theta Rhythm in Humans: Coordinating Self-Directed Hippocampal Learning.
596 *PLoS Biol.* 2012;10: e1001267. doi:10.1371/journal.pbio.1001267

597 14. Ekstrom AD, Caplan JB, Ho E, Shattuck K, Fried I, Kahana MJ. Human Hippocampal Theta
598 Activity During Virtual Navigation. *Hippocampus.* 2005;15: 881–889.
599 doi:10.1002/hipo.20109

600 15. Aghajan ZM, Schuette P, Fields TA, Tran ME, Siddiqui SM, Hasulak NR, et al. Theta
601 Oscillations in the Human Medial Temporal Lobe during Real-World Ambulatory
602 Movement. *Curr Biol.* Elsevier Ltd.; 2017;27: 3743–3751.e3.
603 doi:10.1016/j.cub.2017.10.062

- 604 16. Miller JF, Watrous AJ, Tsitsiklis M, Lee SA, Sheth SA, Schevon CA, et al. Lateralized
605 hippocampal oscillations underlie distinct aspects of human spatial memory and navigation.
606 Nat Commun. Springer US; 2018;9: 2423. doi:10.1038/s41467-018-04847-9
- 607 17. O'Keefe J, Recce ML. Phase Relationship Between Hippocampal Place Units and the EEG
608 Theta Rhythm. *Hippocampus*. 1993;3: 317–330.
- 609 18. Koenig J, Linder AN, Leutgeb JK, Leutgeb S. The spatial periodicity of grid cells is not
610 sustained during reduced theta oscillations. *Science* (80-). 2011;332: 592–595.
611 doi:10.1126/science.1201685
- 612 19. Brandon MP, Bogaard AR, Libby CP, Connerney MA, Gupta K, Hasselmo ME. Reduction
613 of theta rhythm dissociates grid cell spatial periodicity from directional tuning. *Science* (80-
614). 2011;332: 595–600.
- 615 20. Yartsev MM, Witter MP, Ulanovsky N. Grid cells without theta oscillations in the
616 entorhinal cortex of bats. *Nature*. Nature Publishing Group; 2011;479: 103–107.
617 doi:10.1038/nature10583
- 618 21. Herweg NA, Kahana MJ. Spatial representations in the human brain. *Front Hum Neurosci*.
619 2018;
- 620 22. Squire LR, Zola-Morgan S. The Medial Temporal Lobe Memory System. *Science* (80-).
621 1991;253: 1380–1386.
- 622 23. Mayes AR, Montaldi D, Migo E. Associative memory and the medial temporal lobes.
623 *Trends Cogn Sci*. 2007;11: 126–135. doi:10.1016/j.tics.2006.12.003
- 624 24. Eichenbaum H, Yonelinas AP, Ranganath C. The medial temporal lobe and recognition
625 memory. *Annu Rev Neurosci*. 2007;30: 123–152.
- 626 25. Diana RA, Yonelinas AP, Ranganath C. Imaging recollection and familiarity in the medial
627 temporal lobe: A three-component model. *Trends Cogn Sci*. 2007;11: 379–386.
628 doi:10.1016/j.tics.2007.08.001
- 629 26. Wixted JT, Squire LR. The medial temporal lobe and the attributes of memory. *Trends Cogn*
630 *Sci*. Elsevier Ltd; 2011;15: 210–217. doi:10.1016/j.tics.2011.03.005
- 631 27. Wixted JT, Squire LR. The medial temporal lobe and the attributes of memory. *Trends Cogn*
632 *Sci*. Elsevier Ltd; 2011;15: 210–217. doi:10.1016/j.tics.2011.03.005
- 633 28. Buzsáki G. Theta rhythm of navigation: Link between path integration and landmark
634 navigation, episodic and semantic memory. *Hippocampus*. 2005;15: 827–840.
635 doi:10.1002/hipo.20113
- 636 29. Solomon EA, Stein JM, Das S, Gorniak R, Sperling MR, Gross RE, et al. Functional wiring
637 of the human medial temporal lobe. *bioRxiv*. 2018;257899. doi:10.1101/257899
- 638 30. Burke JF, Sharan AD, Sperling MR, Ramayya AG, Evans JJ, Healey MK, et al. Theta and
639 High-Frequency Activity Mark Spontaneous Recall of Episodic Memories. *J Neurosci*.
640 2014;34: 11355–11365. doi:10.1523/JNEUROSCI.2654-13.2014
- 641 31. Weidemann CT, Kragel JE, Lega BC, Worrell GA, Sperling MR, Sharan A, et al. Neural
642 activity reveals interactions between episodic and semantic memory systems during
643 retrieval. 2017; doi:10.1002/(SICI)1097-0169(1999)43:3<255::AID-CM8>3.0.CO;2-T
- 644 32. Kragel JE, Ezzyat Y, Sperling MR, Gorniak R, Worrell GA, Berry BM, et al. Similar

- 645 patterns of neural activity predict memory function during encoding and retrieval.
646 Neuroimage. Elsevier; 2017;155: 60–71. doi:10.1016/j.neuroimage.2017.03.042
- 647 33. Lega BC, Jacobs J, Kahana MJ. Human hippocampal theta oscillations and the formation
648 of episodic memories. *Hippocampus*. 2012;22: 748–761. doi:10.1002/hipo.20937
- 649 34. Herweg NA, Aritz T, Leicht G, Mulert C, Fuentemilla L, Bunzeck N. Theta-alpha
650 oscillations bind the hippocampus, prefrontal cortex, and striatum during recollection:
651 Evidence from simultaneous EEG–fMRI. *J Neurosci*. 2016;36: 3579–3587.
- 652 35. Guderian S, Düzel E. Induced theta oscillations mediate large-scale synchrony with
653 mediotemporal areas during recollection in humans. *Hippocampus*. 2005;15: 901–912.
654 doi:10.1002/hipo.20125
- 655 36. Miller JF, Neufang M, Solway A, Brandt A, Trippel M, Mader I, et al. Neural activity in
656 human hippocampal formation reveals the spatial context of retrieved memories. *Science*
657 (80-). 2013;365: 1111–1114.
- 658 37. Treves A, Rolls ET. Computational analysis of the role of the hippocampus in memory.
659 *Hippocampus*. 1994;4: 374–391. doi:10.1002/hipo.450040319
- 660 38. Solomon EA, Kragel JE, Sperling MR, Sharan A, Worrell G, Kucewicz M, et al.
661 Widespread theta synchrony and high-frequency desynchronization underlies enhanced
662 cognition. *Nat Commun*. Springer US; 2017;8. doi:10.1038/s41467-017-01763-2
- 663 39. Watrous AJ, Tandon N, Conner CR, Pieters T, Ekstrom AD. Frequency-specific network
664 connectivity increases underlie accurate spatiotemporal memory retrieval. *Nat Neurosci*.
665 Nature Publishing Group; 2013;16: 349–356. doi:10.1038/nn.3315
- 666 40. Senior TJ, Huxter JR, Allen K, O’Neill J, Csicsvari J. Gamma Oscillatory Firing Reveals
667 Distinct Populations of Pyramidal Cells in the CA1 Region of the Hippocampus. *J Neurosci*.
668 2008;28: 2274–2286. doi:10.1523/JNEUROSCI.4669-07.2008
- 669 41. Skaggs WE, McNaughton BL, Wilson MA, Barnes CA. Theta phase precession in
670 hippocampal neuronal populations and the compression of temporal sequences.
671 *Hippocampus*. 1996;6: 149–172.
- 672 42. Dragoi G, Buzsáki G. Temporal Encoding of Place Sequences by Hippocampal Cell
673 Assemblies. *Neuron*. 2006;50: 145–157. doi:10.1016/j.neuron.2006.02.023
- 674 43. Lisman JE, Jensen O. The Theta-Gamma Neural Code. *Neuron*. Elsevier Inc.; 2013;77:
675 1002–1016. doi:10.1016/j.neuron.2013.03.007
- 676 44. Fuentemilla L, Penny WD, Cashdollar N, Bunzeck N, Düzel E. Theta-coupled periodic
677 replay in working memory. *Curr Biol*. 2010;20: 606–12. doi:10.1016/j.cub.2010.01.057
- 678 45. Kerrén C, Linde-Domingo J, Hanslmayr S, Wimber M. An Optimal Oscillatory Phase for
679 Pattern Reactivation during Memory Retrieval. *Curr Biol*. 2018;28: 3383–3392.e6.
680 doi:10.1016/j.cub.2018.08.065
- 681 46. Fries P. A mechanism for cognitive dynamics: Neuronal communication through neuronal
682 coherence. *Trends Cogn Sci*. 2005;9: 474–480. doi:10.1016/j.tics.2005.08.011
- 683 47. Cohen MX. Assessing transient cross-frequency coupling in EEG data. *J Neurosci Methods*.
684 2008;168: 494–499. doi:10.1016/j.jneumeth.2007.10.012
- 685 48. Gmeindl L, Walsh M, Courtney SM. Binding serial order to representations in working

- 686 memory: A spatial/verbal dissociation. *Mem Cogn*. 2011;39: 37–46. doi:10.3758/s13421-
687 010-0012-9
- 688 49. Solomon EA, Lega BC, Sperling MR, Kahana MJ. Hippocampal theta codes for distances
689 in semantic and temporal spaces. *bioRxiv*. 2019;611681.
690 doi:http://dx.doi.org/10.1101/611681
- 691 50. Herweg NA, Sharan AD, Sperling MR, Brandt A, Schulze-Bonhage A, Kahana MJ.
692 Reactivated spatial context guides episodic recall. *bioRxiv*. 2018; 399972.
693 doi:10.1101/399972
- 694 51. Vass LK, Copara MS, Seyal M, Shahlaie K, Farias ST, Shen PY, et al. Oscillations Go the
695 Distance: Low-Frequency Human Hippocampal Oscillations Code Spatial Distance in the
696 Absence of Sensory Cues during Teleportation. *Neuron*. Elsevier Inc.; 2016;89: 1180–1186.
697 doi:10.1016/j.neuron.2016.01.045
- 698 52. Miller JF, Watrous AJ, Tsitsiklis M, Lee SA, Sheth SA, Schevon CA, et al. Lateralized
699 hippocampal oscillations underlie distinct aspects of human spatial memory and navigation.
700 *Nat Commun*. Springer US; 2018; doi:10.1038/s41467-018-04847-9
- 701 53. Javadi A-H, Patai EZ, Margois A, Tan H-RM, Kumaran D, Nardini M, et al. Spotting the
702 path that leads nowhere: Modulation of human theta and alpha oscillations induced by
703 trajectory changes during navigation. *bioRxiv*. 2018;301697. Available: [http://e-](http://e-journal.uajy.ac.id/14649/1/JURNAL.pdf)
704 [journal.uajy.ac.id/14649/1/JURNAL.pdf](http://e-journal.uajy.ac.id/14649/1/JURNAL.pdf)
- 705 54. Staresina BP, Cooper E, Henson RNA. Reversible information flow across the medial
706 temporal lobe: The hippocampus links cortical modules during memory retrieval. *J*
707 *Neurosci*. 2013;33: 14184–14192. doi:10.1523/JNEUROSCI.1987-13.2013
- 708 55. Staresina BP, Reber TP, Niediek J, Boström J, Elger CE, Mormann F. Recollection in the
709 human hippocampal-entorhinal cell circuitry. *Nat Commun*. Springer US; 2019;10: 1503.
710 doi:10.1038/s41467-019-09558-3
- 711 56. Moser EI, Kropff E, Moser M-B. Place cells, grid cells, and the brain’s spatial representation
712 system. *Annu Rev Neurosci*. 2008;31: 69–89.
713 doi:10.1146/annurev.neuro.31.061307.090723
- 714 57. Nadasdy Z, Nguyen TP, Török Á, Shen JY, Briggs DE, Modur PN, et al. Context-dependent
715 spatially periodic activity in the human entorhinal cortex. *Proc Natl Acad Sci*. 2017;114:
716 E3516–E3525. doi:10.1073/pnas.1701352114
- 717 58. Lega B, Burke JF, Jacobs J, Kahana MJ. Slow-Theta-to-Gamma Phase – Amplitude
718 Coupling in Human Hippocampus Supports the Formation of New Episodic Memories.
719 *Cereb Cortex*. 2014;26: 268–278. doi:10.1093/cercor/bhu232
- 720 59. Mormann F, Fell J, Axmacher N, Weber B, Lehnertz K, Elger CE, et al. Phase/amplitude
721 reset and theta-gamma interaction in the human medial temporal lobe during a continuous
722 word recognition memory task. *Hippocampus*. 2005;15: 890–900. doi:10.1002/hipo.20117
- 723 60. Friese U, Köster M, Hassler U, Martens U, Trujillo-Barreto N, Gruber T. Successful
724 memory encoding is associated with increased cross-frequency coupling between frontal
725 theta and posterior gamma oscillations in human scalp-recorded EEG. *Neuroimage*.
726 Elsevier Inc.; 2013;66: 642–647. doi:10.1016/j.neuroimage.2012.11.002
- 727 61. Tort ABL, Komorowski RW, Manns JR, Kopell NJ, Eichenbaum H. Theta-gamma coupling

- 728 increases during the learning of item-context associations. *Proc Natl Acad Sci.* 2009;106:
729 20942–20947. doi:10.1073/pnas.0911331106
- 730 62. Igarashi KM, Lu L, Colgin LL, Moser MB, Moser EI. Coordination of entorhinal-
731 hippocampal ensemble activity during associative learning. *Nature.* 2014;510: 143–147.
732 doi:10.1038/nature13162
- 733 63. Solway A, Miller JF, Kahana MJ. PandaEPL: A library for programming spatial navigation
734 experiments. *Behav Res Methods.* 2013;45: 1293–1312. doi:10.3758/s13428-013-0322-5
- 735 64. Avants BB, Epstein CL, Grossman M, Gee JC. Symmetric diffeomorphic image registration
736 with cross-correlation: Evaluating automated labeling of elderly and neurodegenerative
737 brain. *Med Image Anal.* 2008;12: 26–41. doi:10.1016/j.media.2007.06.004
- 738 65. Gramfort A, Luessi M, Larson E, Engemann DA, Strohmeier D, Brodbeck C, et al. MNE
739 software for processing MEG and EEG data. *Neuroimage.* Elsevier Inc.; 2014;86: 446–460.
740 doi:10.1016/j.neuroimage.2013.10.027
- 741